Supporting Information for

DMSO Affects $A\beta_{1-40}$'s Conformation and Interactions with Aggregation Inhibitors as Revealed by NMR

Douglas V. Laurents, David Pantoja-Uceda, Laura C. López, José Alberto Carrodeguas, Miguel Mompeán, Mª Ángeles Jiménez, Javier Sancho

Detailed Experimental Procedures

Supporting Table 1: Summary of NMR Experiments.

Supporting Table 2: ^{1}H, ^{13}C, ^{15}N assignments of $A\beta_{1-40}$ in $DMSO_{d6}$ at 30 ºC.

Supporting Table 3: $A\beta_{1-40}$ Calculated Intrinsic Hydrogen/Deuterium Exchange.

Sup. Fig. 1 ^{1}H-^{15}N Spectra of $A\beta_{1-40}$ in water/DMSO mixtures.

Sup. Fig. 2 Inter-residual correlations from the 3D HNCACB spectrum.

Sup. Fig. 3 Assigned ^{1}H-^{13}C HSQC of $A\beta_{1-40}$.

Sup. Fig. 4 Comparison of chemical shift values of $A\beta_{1-40}$ (this work) and $A\beta_{1-28}$ (Sorimachi, K. & Craik D. J. (1994)) in DMSO.

Sup. Fig. 5 2D ^{1}H NOESY spectrum of $A\beta_{1-40}$ in $DMSO_{d6}$.

Sup. Fig. 6. ^{1}H-^{15}N HSQC spectra of $A\beta_{1-40}$ with and with heteronuclear NOE.

Sup. Fig. 7 Comparsion of ^{1}H-^{15}N NOE ratio of $A\beta_{1-40}$ in water and $DMSO_{d6}$.

Sup. Fig. 8 H/D exchange of Aβ preincubated in DMSO.

Sup. Fig. 9 ThT Assay of Aβ incubated in DMSO or aqueous solution.

Sup. Fig. 10 1D ^{1}H NMR spectra of Aβ and Inhibitor Compounds.

Sup. Fig. 11 2D ^{1}H-^{15}N HSQC NMR spectra of Aβ alone and titrated with C1 in aqueous solution or $DMSO_{d6}$.

Sup. Fig. 12. ^{1}H-^{15}N Aβ Chemical Shift Changes Induced by C2 (**A**), C3 (**B**) and C4 (**C**) in $DMSO_{d6}$

DETAILED EXPERIMENTAL PROCEDURES

NMR assignment: $A\beta_{1\text{-}40}$, $^{15}N\text{-}A\beta_{1\text{-}40}$ and $^{13}C,^{15}N\text{-}A\beta_{1\text{-}40}$ samples were purchased from rPeptide (Georgia, USA). Deuterated $DMSO_{d6}$ (99% atom D), in ampules, was obtained from Sigma/Aldrich. The $^{13}C,^{15}N\text{-}A\beta_{1\text{-}40}$ sample used for assignment was prepared at 100 μM protein concentration by dissolving the lyophilized material in 220 μl of $DMSO_{d6}$. The use of a 5mm diameter DMSO-matched Shigemi tube reduced the expense of $^{13}C,^{15}N\text{-}A\beta_{1\text{-}40}$ and allowed us to avoid the presence of an air-solvent interface. All NMR experiments for assignment were performed on a Bruker AV spectrometer, operating at 800.1 MHz (^{1}H), and equipped with a cryogenically cooled triple-resonance (^{1}H, ^{13}C, ^{15}N) TCI probe head to improve the signal/noise and pulsed z-field gradients. For sequential assignment, a suite of triple resonance NMR spectra were recorded: 3D HNCO, HNCA, HNCA-intra, HNCACB, CBCA(CO)NH, (H)CC(CO)NH and H(CCCO)NH. These were complemented with the acquisition of several experiments $^{1}H\text{-}^{15}N$ HSQCs for amino acid type discrimination [1,2]. Furthermore, an alternative approach based on the collect of reduced dimensionality (4,2)D HN(COCA)NH experiment [3] was used to speed up the sequential assignment process. Additionally, to complete the assignment of the $^{13}C,^{15}N\text{-}A\beta_{1\text{-}40}$ protein, 2D $^{1}H\text{-}^{1}H$ TOCSY, $^{1}H\text{-}^{1}H$ NOESY, $^{1}H\text{-}^{13}C$ HSQC, 3D $^{1}H\text{-}^{15}N$ NOESY-HSQC and $^{1}H\text{-}^{13}C$ NOESY-HSQC spectra was recorded. The acquisition parameters of these spectra are given in **Sup. Table 1**. Spectra of $^{13}C,^{15}N\text{-}A\beta_{1\text{-}40}$ in neat $DMSO_{d6}$ were recorded at 30 ºC. In contrast, spectra of $^{13}C,^{15}N\text{-}A\beta_{1\text{-}40}$ (100 μM) in 90%:10%::H_2O:D_2O containing 10 mM K_2HPO_4/KH_2PO_4 pH 7 or $DMSO_{d6}$/aqueous buffer mixtures were recorded at 5 ºC.

Spectra were processed and transformed with TOPSPIN2.1 (Bruker Biospin) and NMRPipe [4]. Spectra were assigned manually with the aid of the SPARKY program and the (4,2)D HN(COCA)N(H) experiment was analyzed using in-house programs. The assignment was confirmed using the automatic approach MARS [5].

Chemical shift referencing: The use of DSS as the internal chemical shift reference in samples containing Aβ is not recommended because Aβ binds DSS and their union could affect Aβ's conformation and DSS's chemical shift [6]. Instead, we used a value of 2.49 ppm for the residual ^{1}H signal of $DMSO_{d6}$ for samples prepared in neat $DMSO_{d6}$ [7]. Based on this ^{1}H reference, the ^{13}C and ^{15}N chemical shifts could be referenced indirectly by multiplying by their gyromagnetic ratios with respect to ^{1}H [8]. In the case of ^{13}C, the values obtained were corroborated by checking the value (39.5 ppm) of the DMSO ^{13}C signal. For samples containing a minor fraction of DMSO in aqueous solution, we found, using a blank containing ca. 10% DMSO, 10% D_2O, 80 % H_2O, 50 microM DSS and no Aβ, that the residual ^{1}H signal of $DMSO_{d6}$ is 2.67 ppm at 5 ºC. This value agrees reasonably well with the published value of 2.71 ppm obtained for traces of $DMSO_{d6}$ in D_2O at 24 ºC [7].

Chemical Shift Analysis: Prediction of secondary structure and backbone dynamics [9] based on ^{1}H, ^{13}C and ^{15}N chemical shifts was performed utilizing the TALOS-N program suite [10].

^{15}N Relaxation: (^{1}H)-^{15}N NOE spectrum[11] for $A\beta_{1-40}$ in $DMSO_{d6}$ was acquired at 800 MHz and 30 ºC on a 100 μM uniformly ^{15}N-labeled sample. To measure the backbone ^{1}H-^{15}N NOE ratio, spectral increment in the ^{15}N dimension with and without ^{1}H saturation were recorded in an interleaved fashion and divided during processing into two spectra. The experiments were carried out with an overall recycling delay of 10 s. This experiment provide information on the ps-ns backbone motions [12].

H/X exchange experiment: To test if $A\beta_{1-40}$ in DMSO adopts stable secondary structure, 11 μL of 10 μg/μL ^{15}N-$A\beta_{1-40}$ were diluted ten-fold from $DMSO_{d6}$ into D_2O containing 10 mM $NaAc_{d3}$/DAc_{d3} buffer (final pH 4.52). The exchange of amide protons with solvent deuterons was measured at 5 ºC using a ^{15}N-labeled sample. NMR data acquisition was started within about 15 min of the initiation of the exchange reaction. A series of SOFAST ^{1}H-^{15}N HMQC[13] spectra (relaxation delay of 0.2 s and pulse centered at 8.00 ppm, 768 complex data points, 32 *t*1 increments, 64 scans per increment) were collected over the course of three hours. The acquisition time for each experiment was 9 min. All the spectra

were processed with NMRPipe [17] using the same processing scheme and parameters. The solutions, pipette tips and NMR tube had been precooled in a refrigerator (4 ºC). The shim of the magnet, lock and tuning had been previously optimized using an identical sample.

Thioflavin T (ThT) fluorescence Assay for formation of amyloid-like structure: ThT fluorescence assays were performed following the protocol described by LeVine [14]. Stock solution of ThT (Sigma, St. Louis, USA) was prepared in 3 mM KH_2PO_4/K_2HPO_4 buffer, pH 6.8, to a final concentration of 1 mM. $A\beta_{1-40}$ peptide (rPeptide) was dissolved in both water and DMSO (0.2 mM) and incubated overnight at room temperature. The next morning, they were vortexed just before initiating the experimental measurements with time = 0 being defined as the moment of vortexing. The samples were then incubated and aliquots were taken every two hours to prepare the final samples used for the ThT assay. These samples contained 50 μM ThT and 25 μM in $A\beta_{1-40}$ in each of the solvents; namely, water and DMSO. Spectra were recorded at 30 ºC on a Jobin-Yvon Fluoromax-4 instrument. The excitation wavelength was 440 nm and emission was recorded over 460-500 nm at a scan speed of 0.2 nm s^{-1}, using a slit width of 3 nm for both excitation and emission.

Binding studies with the inhibitor compounds: 1D ^{1}H and 2D ^{1}H-^{13}C HSQC spectra were recorded on the four inhibitor compounds, compound one (C1) = 2-methyl-5,6,7,8-tetrahydro-4H-[1]benzothieno[2,3-d][1,3]oxazin-4-one, compound two (C2)= 2,5-dichloro-N-(4-piperidinophenyl)-3-thiophenesulfonamide, compound three (C3)= N-(4-chloro-2-nitrophenyl)-N'-phenylurea and compound four (C4) = 6-[(4-chlorophenyl)sulfonyl]-2-phenylpyrazolo[1,5-a]pyrimidin-7-amine, either dissolved in water (compound 1) or neat $DMSO_{d6}$ (compounds 1-4) to confirm their identify and assess their purity.

To determine the regions in Aβ affected by inhibitor binding, ^{1}H-^{15}N HSQC spectra were recorded on ^{15}N-$A\beta_{1-40}$ samples (concentration 100 μM) in either 10% $DMSO_{d6}$, 80% H_2O, 10% D_2O with 10 mM KH_2PO_4/K_2HPO_4 pH 7 buffer (for C1) or neat $DMSO_{d6}$ (for C1, C2,

C3 and C4), in the absence or the presence of 1 eq, 3 eq and 5 eq of inhibitor. To analyze ^{1}H-^{15}N HSQC spectra of ^{15}N-Aβ_{1-40} in aqueous solution, we used the assignments reported by the Zagorski[15] and Gräslund[16] laboratories and recently corroborated and extended by Martins et al.[17]. This report corroborates and is more complete than previous studies. Spectra were recorded at 5º C (aqueous solutions) or 30ºC (neat $DMSO_{d6}$) on a Bruker 600 MHz (^{1}H) instrument. Chemical shift changes were determined using the Bruker TOPSPIN 2.1 program, and reported as the weighted mean change of the ^{1}H and ^{15}N nuclei as calculated using the equation:

$$\Delta\delta \text{ (weighted mean} = \sqrt{\{ (\delta\, ^{1}H+C - \delta\, ^{1}H)^2 + ((\delta^{15}N+C - \delta\, ^{15}N)^2/25) \}} \quad \text{(eqn 1)}$$

where $\delta\, ^{1}H+C$ and $\delta\, ^{15}N+C$ are the chemical shift values in the presence of inhibitor compound. It is important to point out that these spectra detect monomeric ^{15}N-Aβ_{1-40} and the smallest oligomers and that larger aggregates are invisible to liquid state NMR spectroscopy.

Supporting References:

1. Pantoja-Uceda, D.; Santoro, J. *J Magn Reson.* **2008**, *195,* 187-195
2. Pantoja-Uceda, D.; Santoro, J. *J Biomol NMR* **2012**, *54,* 145–153
3. Pantoja-Uceda, D.; Santoro, J. *J. Biomol. NMR* **2009**, *45,* 351-356
4. Delaglio, F.; Grzesiek, S.; Vuister, G. W.; Zhu, G.; Pfeifer, J.; Bax, A. *J. Biomol. NMR* **1995**, *6,* 277–293
5. Jung, Y. S.; Zweckstetter, M. *J. Biomol. NMR* **2004**, *30,* 11-23
6. Laurents, D. V.; Gorman, P. M.; Guo, M.; Rico, M.; Chakrabartty, A.; Bruix, M. *J. Biol. Chem.* **2005**, *280,* 3675-3685
7. Gottlieb, H. E.; Kotlyar, V.; Nudelman, A. *J. Org. Chem.* **1997**, *62,* 7512-7520
8. Markley, J. L.; Bax, A.; Arata, Y.; Hilbers, C. W.; Kaptein, R.; Sykes, B. D.; Wright, P. E.; Wüthrich, K. *Pure Appl. Chem.* **1998**, *70,* 117-142
9. Berjanski, M. V.; Wishart, D. S. *J. Am. Chem. Soc.* **2005**, *127,* 14970-14971
10. Shen, Y.; Bax, A. *J. Biomol. NMR* **2013**, *56,* 227-241
11. Farrow, N. A.; Muhandiram, R.; Singer, A. U.; Pascal, S. M.; Kay, C. M.; Gish, G.; Shoelson, S. E.; Pawson, T.; Forman-Kay, J. D.; Kay, L. E. *Biochemistry* **1994**, *33,* 5984–6003
12. Palmer, A. G. *Chemical Reviews* **2004**, *104,* 3623-3640
13. Schanda, P.; Brutscher, B. *J. Am. Chem. Soc.* **2005**, *127,* 8014-8015
14. LeVine, H. I. *Prot Sci* **1993**, *404-410,*
15. Hou, L.; Shao, H.; Zhang, Y.; Li, H.; Memon, N. K.; Neuhaus, E. G.; Brewer, J. M.; Byeon, I.-J. L.; Ray, D. G.; Vitek, M. P.*, et al. J. Am. Chem. Soc.* **2004**, *126,* 1992-2005

16. Danielsson, J.; Andersson, A.; Jarvet, J.; Gräslund, A. *Mag. Res. Chem.* **2006**, *44,* S114-S121
17. Martins, A. F.; Dias, D.; Morfin, J. F.; Lacerda, S.; Laurents, D. V.; Töth, E.; Geraldes, C. F. G. C. *Chem. Eur. J.* **2015**, *doi:10.1002/chem.201406152,*

Supporting Table 1: NMR Spectral Acquisition.

TYPE OF SPECTRUM	# SCANS	MATRIX	SWEEP WIDTH (ppm) / **mixing time** (ms)
1D 1H	32	32k	12
2D TOCSY	16	2k x 512	10 x 10 / **60**
2D NOESY	64 - 80	2k x 512	10 x 10 / **150**
2D ^{1}H-^{15}N HSQC	8	2k x 256	12 x 20
2D ^{1}H-^{15}N HSQC*	16	2k x 288	12 x 8.9
2D ^{1}H-^{13}C HSQC	8	2k x 256	8 x 60
3D ^{1}H-^{15}N NOESY-HSQC	16	2k x 64 x 96 1H 15N 1H	12 x 22 x 12 / **150** 1H 15N 1H
3D ^{1}H-^{13}C NOESY-HSQC	32	2k x 64 x 80 1H 13C 1H	13 x 56 x 13 / **150** 1H 13C 1H
3D HNCO	4	2k x 32 x 90 1H 15N 13C	9 x 8.9 x 22.1 1H 15N 13C
3D CBCA(CO)NH	8	2k x 32 x 100	9 x 8.9 x 7.5
3D HNCABCB	16	2k x 32 x 100	9 x 8.9 x 75
3D HNCA-intra	8	2k x 32 x 90	9 x 8.9 x 32
3D HNCA	8	2k x 32 x 90	9 x 8.9 x 32
3D (H)CC(CO)NH	8	2k x 32 x 128 1H 15N 13C	9 x 8.9 x 75 1H 15N 13C
3D H(CCCO)NH	8	2k x 32 x 110 1H 15N x 1H	9 x 8.9 x 12 1H 15N 1H
(4,2)D HN(COCA)NH	8	2k x 512 $^{1}H_{i}$($\sum^{1}H_{j}$,$^{15}N_{i}$,$^{15}N_{j}$)	9 x 40 $^{1}H_{i}$ ($\sum^{1}H_{j}$,$^{15}N_{i}$,$^{15}N_{j}$)
2D ^{1}H-^{15}N HSQC with or without NOE	8	2k x 256	10 x 20 / relaxation delay = 10 s
2D^{1}H-^{15}N SOFAST HMQC (to monitor H/D exchange)	64 / aqc. Time = 10 min.	768 x 32	14 x 23 / relaxation delay = 0.2 s

*^{1}H-^{15}N HSQC for amino acid type discrimination, see Pantoja-Uceda & Santoro (2008); Pantoja-Uceda & Santoro (2012).

Supporting Table 2: ^{1}H, ^{13}C, ^{15}N assignments of $A\beta_{1-40}$ in $DMSO_{d6}$ at 30 ºC.

	N	HN	HA	HB	HG	HD	HE	HZ	CO	CA	CB	CG	CD	CE
D1			4.050	2.775, 2.610	-	-	-		170.7	51.99	38.88	-	-	-
A2	121.9	8.57	4.292	1.156	-	-	-		174.6	51.34	20.99	-	-	-
E3	116.2	8.01	4.175	1.803, 1.660	2.147	-	-		174.0	55.03	30.48	33.23	-	-
F4	116.5	7.87	4.442	2.859, 2.588	-	7.23	7.36	7.30	174.3	57.18	39.91	-	-	-
R5	117.8	8.17	4.252	1.521, 1.434	1.668	3.06	-		174.2	55.29	32.02	28.02	43.50	-
H6	117.1	8.13	4.530	3.00, 2.90	-	-	-		173.3	54.89	31.0	-	-	-
D7	118.3	8.36	4.573	2.688, 2.614	-	-	-		173.9	52.42	39.24	-	-	-
S8	113.5	8.13	4.238	3.594	-	-	-		173.3	58.42	64.63	-	-	-
G9	106.7	8.06	3.688	-	-	-	-		171.6	44.91	-	-	-	-
Y10	116.3	7.94	4.516	2.765, 2.698	-	7.01	6.64		174.3	56.41	40.38	-	-	-
E11	118.2	8.20	4.287	1.876, 1.733	2.219	-	-		174.3	55.02	30.25	33.39	-	-
V12	115.5	7.71	4.122	1.92	0.80, 0.78	-	-		174.0	60.81	33.6	22.2, 21.0	-	-
H13	119.6	8.16	4.489	3.00, 2.90	-	-	-			55.30	31.0	-	-	-
H14			4.489	3.00, 2.90	-	-	-		173.3	55.46	31.0	-	-	-
Q15	118.7	8.36	4.188	1.80	2.070	-	-		174.2	55.02	30.99	34.52	-	-
K16	118.6	8.21	4.226	1.614	1.269	1.469	2.72		174.3	55.28	34.26	25.20	29.69	41.8
L17	119.4	7.90	4.298	1.384, 1.331	1.517	0.81; 0.76	-		174.7	53.95	43.58	27.31	26.1, 24.7	-
V18	115.2	7.64	4.054	1.81	0.68	-	-		173.5	60.56	33.8	22.2, 21.1	-	-
F19	118.9	7.88	4.497	2.927, 2.695	-	7.18	7.36 -	7.30	173.8	56.58	40.61	-	-	-
F20	116.9	8.05	4.533	2.987, 2.776	-	7.24	7.36	7.30	173.6	56.57	40.47	-	-	-
A21	121.2	8.12	4.300	1.192	-	-	-		175.0	51.18	21.08	-	-	-
E22	115.5	7.97	4.277	1.869, 1.721	2.219	-	-		174.1	54.65	30.81	33.03	-	-
D23	118.1	8.22	4.575	2.693	-	-	-		173.4	52.65	38.64	-	-	-
V24	114.1	7.64	4.125	1.92	0.80, 0.78	-	-		173.1	60.82	33.6	22.2, 21.0	-	-
G25	107.6	8.09	3.709	-	-	-	-		171.8	44.87	-	-	-	-
S26	112.5	7.92	4.329	3.524	-	-	-		173.1	57.71	64.87	-	-	-
N27	119.3	8.21	4.524	2.853, 2.567	-	-	-		174.0	52.86	39.73	-	-	-
K28	117.4	7.95	4.132	1.687	1.301	1.47	2.72		174.8	55.69	33.80	25.07	29.55	41.8
G29	105.7	8.09	3.624	-	-	-	-		171.3	44.95	-	-	-	-
A30	119.7	7.83	4.313	1.157	-	-	-		175.2	51.00	21.27	-	-	-
I31	115.6	7.87	4.133	1.708	1.40, 1.05; 0.77	0.77	-		173.9	60.00	39.20	27.4; 18.44	14.08	-
I32	118.7	7.69	4.144	1.699	1.40, 1.05; 0.79	0.77	-		174.1	59.91	39.66	27.4; 18.35	14.08	-
G33	108.3	8.06	3.641	-	-	-	-		171.4	44.95	-	-	-	-
L34	118.0	7.85	4.309	1.426, 1.382	1.545	0.84; 0.80	-		175.1	54.01	44.13	27.04	26.1 24.7	-
M35	118.4	8.13	4.330	1.888, 1.773	2.36, 2.42	-	2.00		174.0	54.95	34.49	32.6	-	17.8
V36	114.7	7.60	4.119	1.92	0.80, 0.78	-	-		174.1	60.65	33.6	22.2, 21.0	-	-
G37	108.0	8.16	3.780	-	-	-	-		171.9	44.88	-	-	-	-
G38	105.0	8.00	3.723	-	-	-	-		171.5	44.87	-	-	-	-
V39	114.0	7.76	4.302	2.01	0.86	-	-		174.2	60.15	32.6	22.2, 21.3	-	-
V40	117.0	7.98	4.056	1.82	0.68	-	-			60.34	33.8	22.2, 21.1	-	-

Supporting Table 3: $A\beta_{1-40}$ Calculated Intrinsic Hydrogen/Deuterium Exchange and Experimentally Determined Protection Factors (pH* 4.52, 5ºC).

Residue	H/X Intrinsic Lifetime (min)[a]	Protection Factor	Residue H/X Intrinsic Lifetime (min)	H/X Intrinsic Lifetime (min)[a]	Protection Factor
Asp 1	- - -	- - -	Ala 21	5.08	3.1
Ala 2	0.176	91	Glu 22	11.1	1.4
Glu 3	11.1	1.5	Asp 23	8.30	1.9
Phe 4[b]	**9.69**	**7 ± 5**	Val 24	27.2	0.57
Arg 5	4.26	3.8	Gly 25	4.35	3.7
His 6	0.621	26	Ser 26	1.74	9.2
Asp 7	1.39	12	Asn 27	0.984	16.3
Ser 8	3.03	5.3	Lys 28	3.12	5.1
Gly 9	1.62	9.9	Gly 29	2.44	6.6
Tyr 10	7.18	2.2	Ala 30	3.98	4.0
Glu 11	10.0	1.6	**Ile 31**	**25.1**	**17 ± 8**
Val 12	23.8	0.7	**Ile 32**	**36.5**	**6.9 ± 0.6**
His 13	1.41	11.3	Gly 33	5.30	3.0
His 14	0.161	99	**Leu 34**	**13.7**	**3.9 ± 1.5**
Gln 15	0.824	4	Met 35	9.27	1.7
Lys 16	4.07	1.1	Val 36	19.4	0.82
Leu 17	15.1	1.1	Gly 37	4.35	3.7
Val 18	33.8	0.5	Gly 38	2.18	7.3
Phe 19	12.9	1.2	Val 39	17.3	0.92
Phe 20	8.52	1.9	**Val 40**	**99.4**	**1.8 ± 0.2**

[a] Calculated on the basis of the polypeptide sequence using the nearest neighbor parameters of Bai *et al* (1993) and the temperature of 5 ºC and the final pH* of 4.52.

[b] Residues with observed slow exchange and calculated protection factors are shown in bold. For the remaining residues, the protection factors shown are the upper limits calculated on the basis of the experimental dead time (16 minutes) and each HN group's intrinsic exchange lifetime.

Sup. Fig. 1 ^{1}H-^{15}N HSQC Spectra of $A\beta_{1\text{-}40}$ in water/DMSO mixtures.

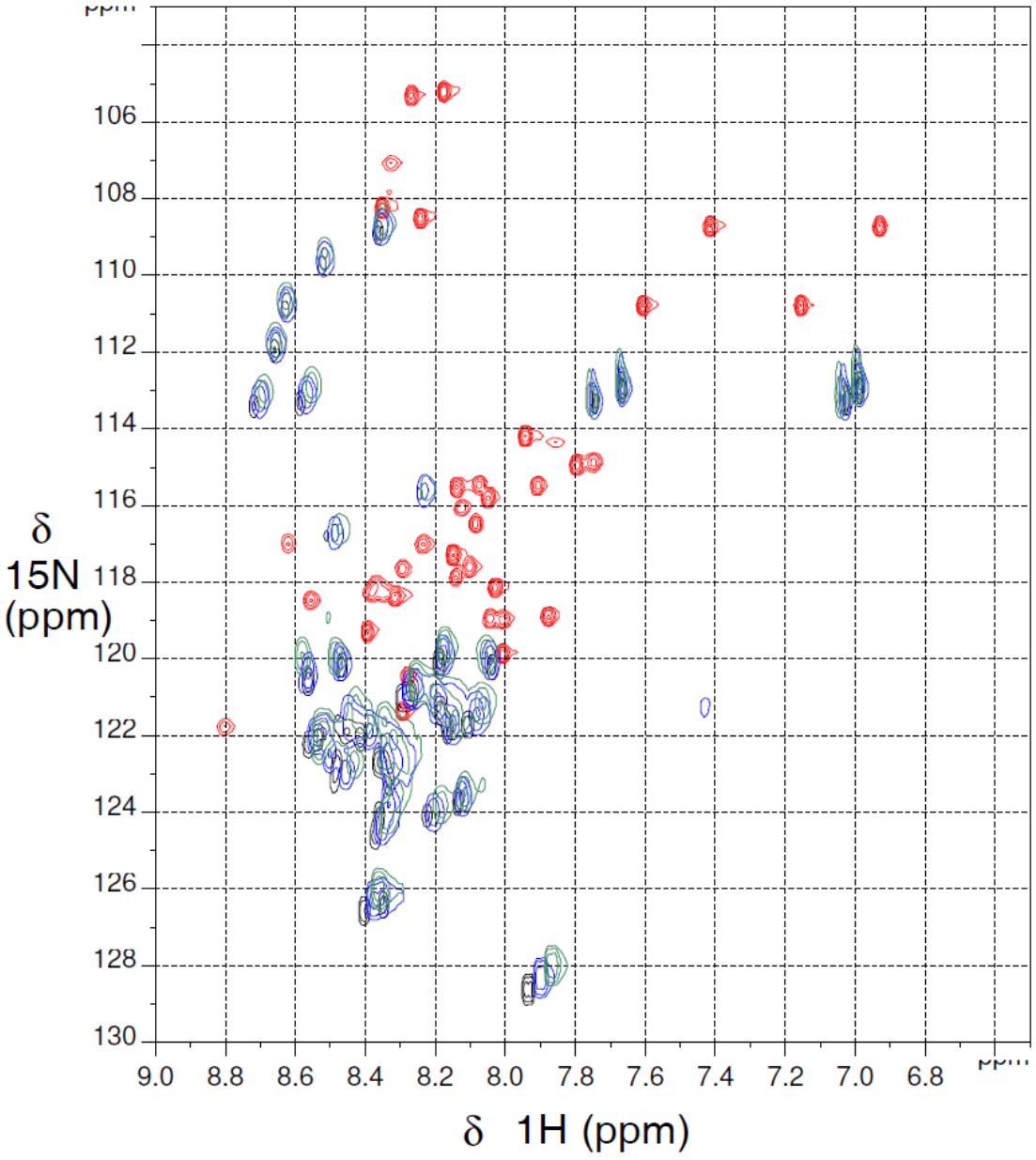

$A\beta_{1\text{-}40}$ in H_2O (**black**), 1:16::DMSO $_{d6}$:H_2O (**blue**), 1:8::$DMSO_{d6}$:H_2O (**green**), 100% DMSO $_{d6}$ (**red**). The chemical shift perturbations induced by $DMSO_{d6}$ are -1.3 ± 1.7 ppB /% $DMSO_{d6}$ for ^{1}HN and 27 ± 11 ppB / % $DMSO_{d6}$ for ^{15}N over the range of 0 – 12.5 % $DMSO_{d6}$. V40 ($^{1}H\delta$ = 7.92 ppm, $^{15}N\delta$ = 128.7 ppm in H_2O and $^{1}H\delta$ = 7.98 ppm, $^{15}N\delta$ = 117.0 ppm in 100% $DMSO_{d6}$), which is the residue most affected by low amounts of DMSO (-5.4 ppB/%$DMSO_{d6}$ for ^{1}HN and -50 ppB / %$DMSO_{d6}$ for ^{15}N), is also the residue whose HN resonances differ the most in aqueous solution vs. 100% $DMSO_{d6}$.

Sup. Fig. 2 "Strip" plot showing representative inter-residual correlations based on the 3D HNCACB spectrum.

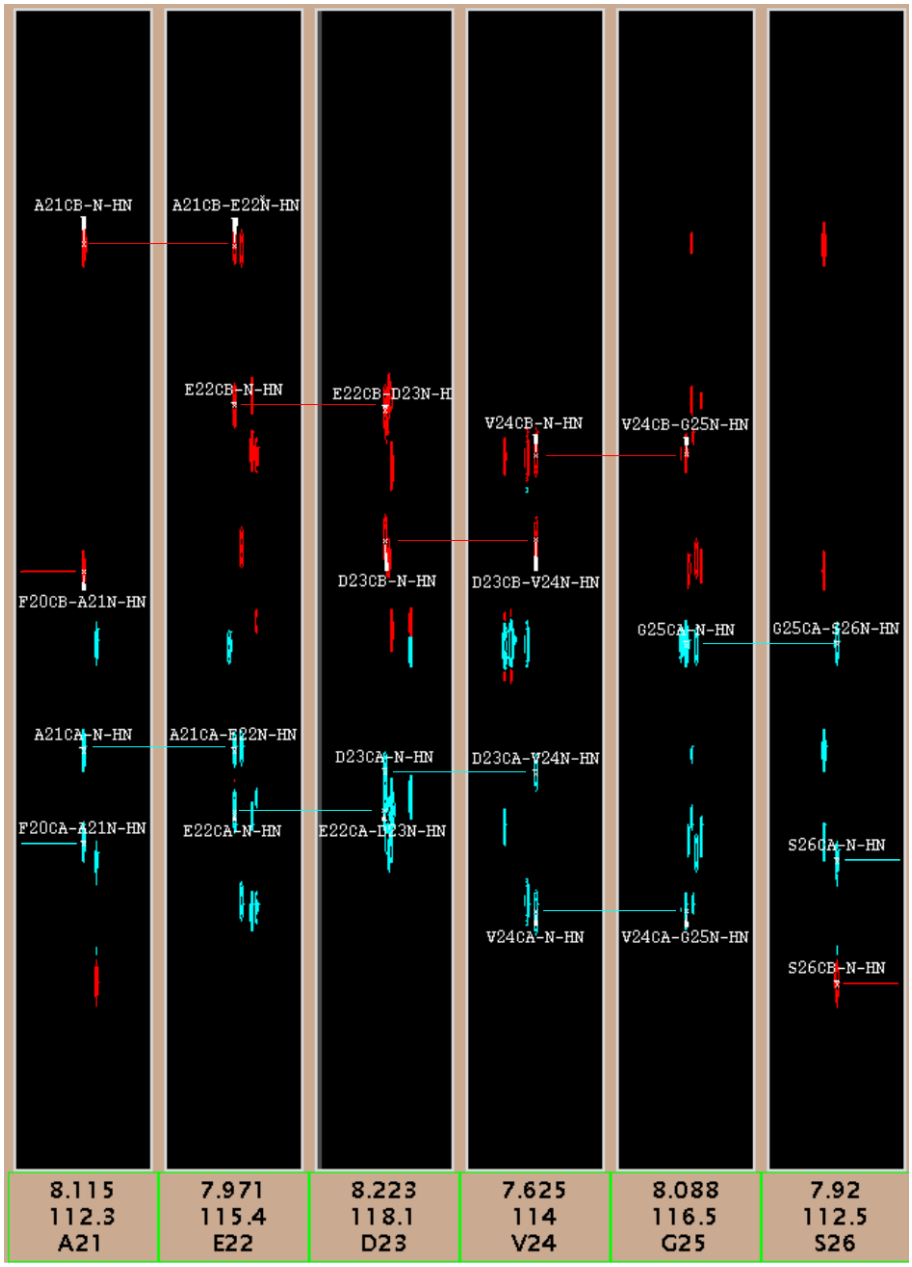

Three positive (**cyan**) and three negative (**red**) contours are plotted. Note that in this spectrum, Cα resonances appear as positive signals while Cβ signals are negative. The ^{13}C chemical shift, plotted on the y-axis ranges from 4.5 ppm (*top*) to 79 ppm (*bottom*). The ^{1}H, ^{15}N chemical shifts and residue identity are indicated at the bottom of the graph. Due to spectral folding to optimize acquisition time and sensitivity, the ^{15}N chemical shifts of A21 and G25 are displaced.

Sup. Fig. 3 ^{1}H-^{13}C HSQC of $A\beta_{1\text{-}40}$ Panel **A**, Alpha region

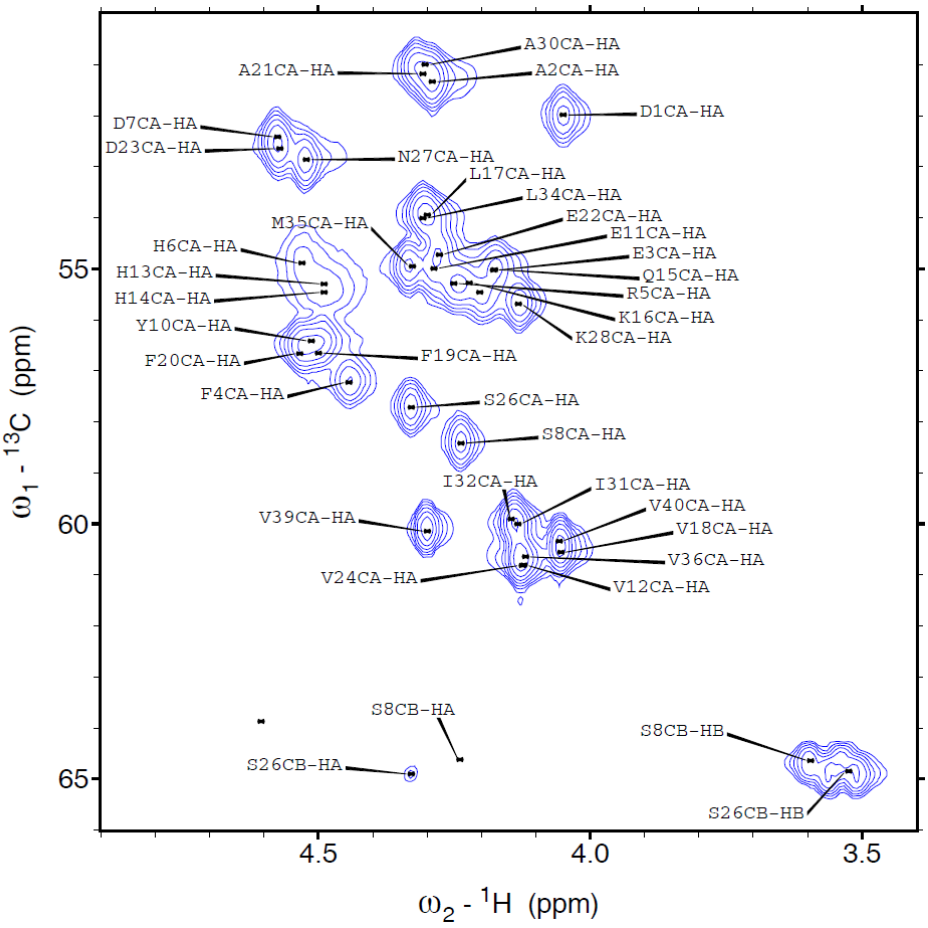

Sup. Fig. 3 (cont.) ^{1}H-^{13}C HSQC of $A\beta_{1-40}$ Panel **B**, Side chain Region.

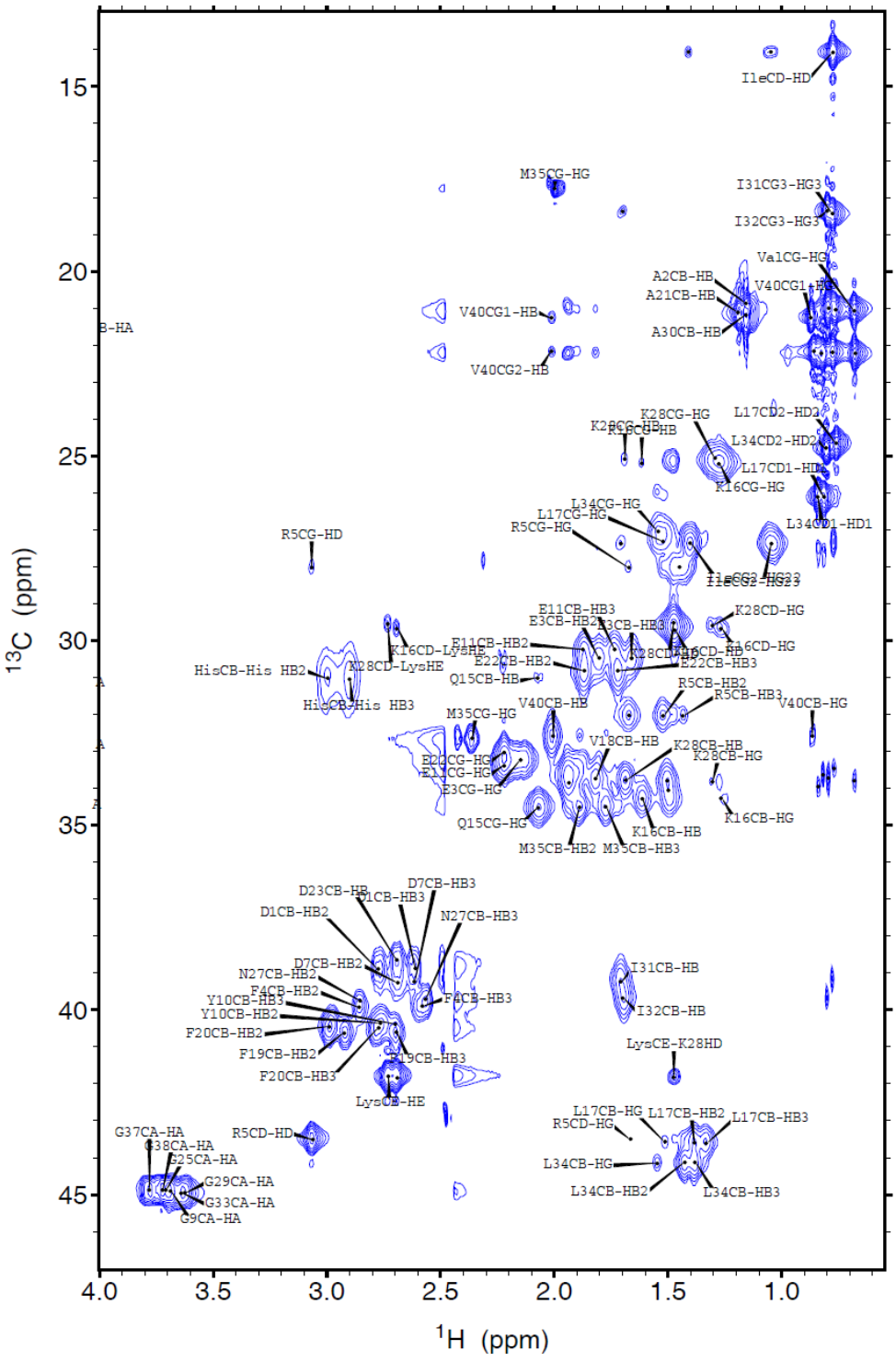

Sup. Fig. 4: Comparison of chemical shift values of $A\beta_{1\text{-}40}$ (this work) and $A\beta_{1\text{-}28}$ {Sorimachi, K. & Craik D. J. (1994)} in DMSO.

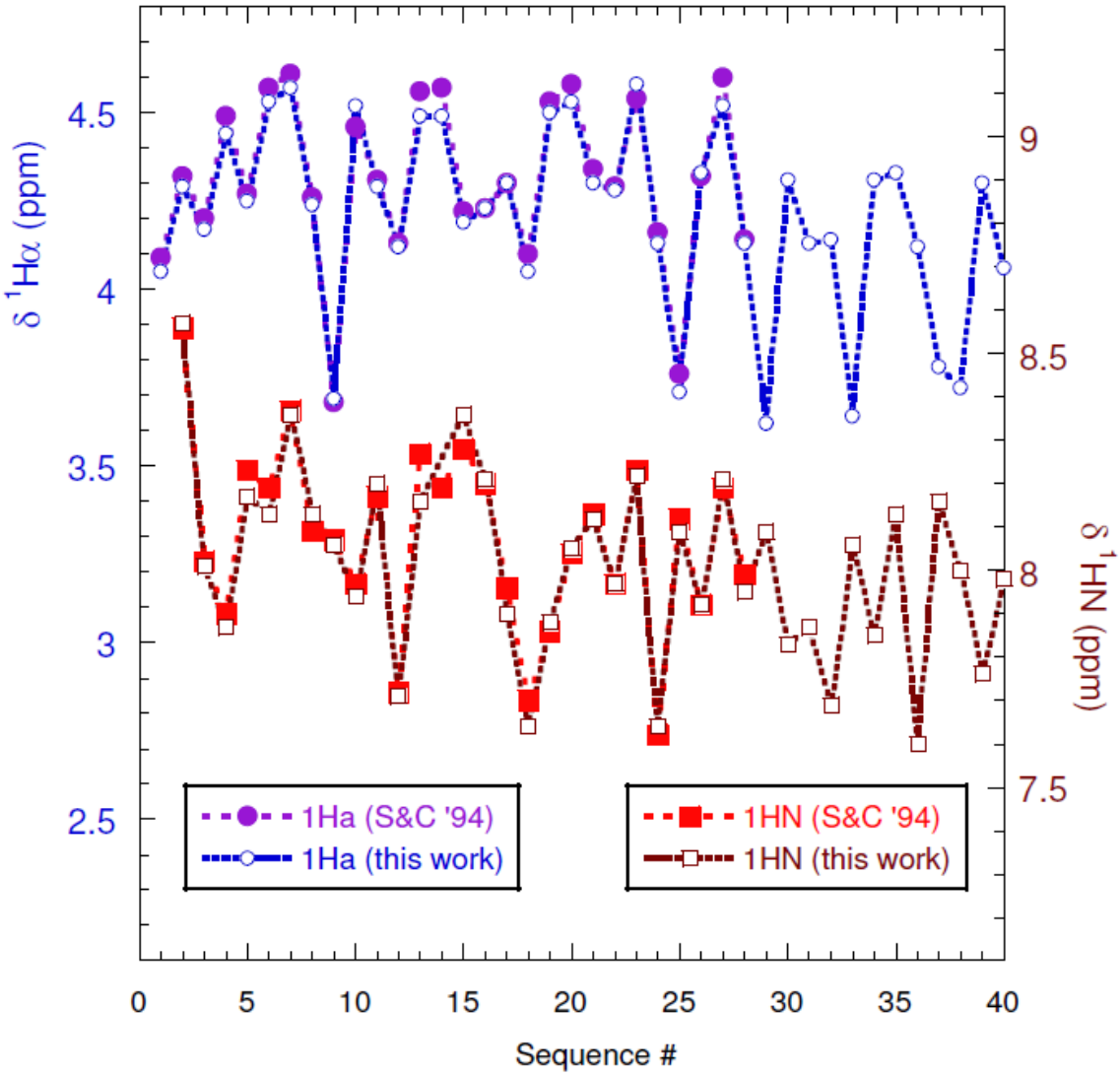

Left y-axis, $^{1}H\alpha$ chemical shift values, right y-axis, ^{1}HN chemical shifts.

Sup. Fig. 5: 2D ^{1}H-^{1}H NOESY spectrum of $A\beta_{1\text{-}40}$ in $DMSO_{d6}$.

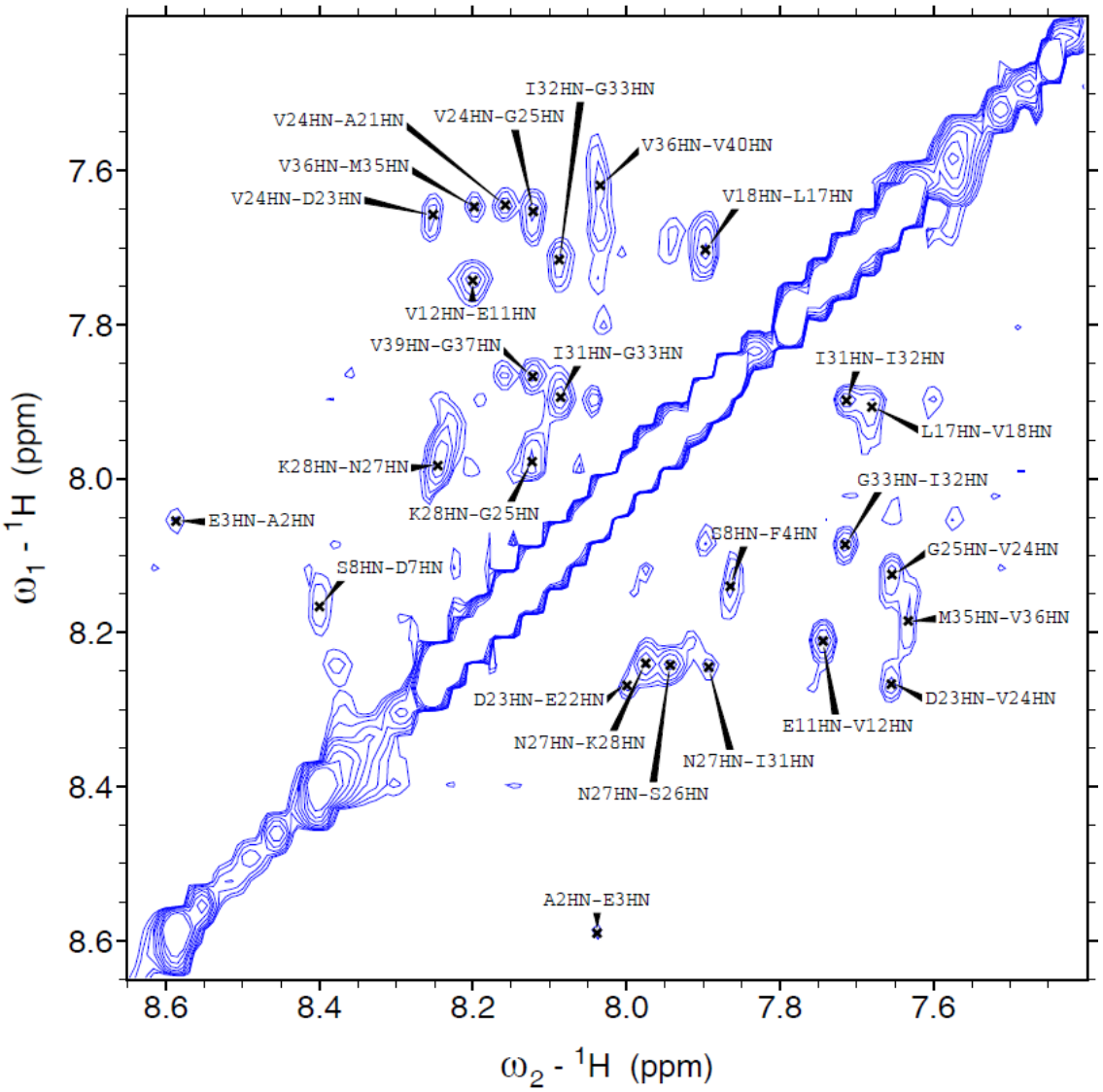

Peaks which could be unambiguously assigned are labeled. Contour base is 120000 and the multiplication factor between contours is 1.5 x.

Sup. Fig. 6. ^{1}H-^{15}N HSQC spectra of $A\beta_{1\text{-}40}$ without and with heteronuclear NOE.

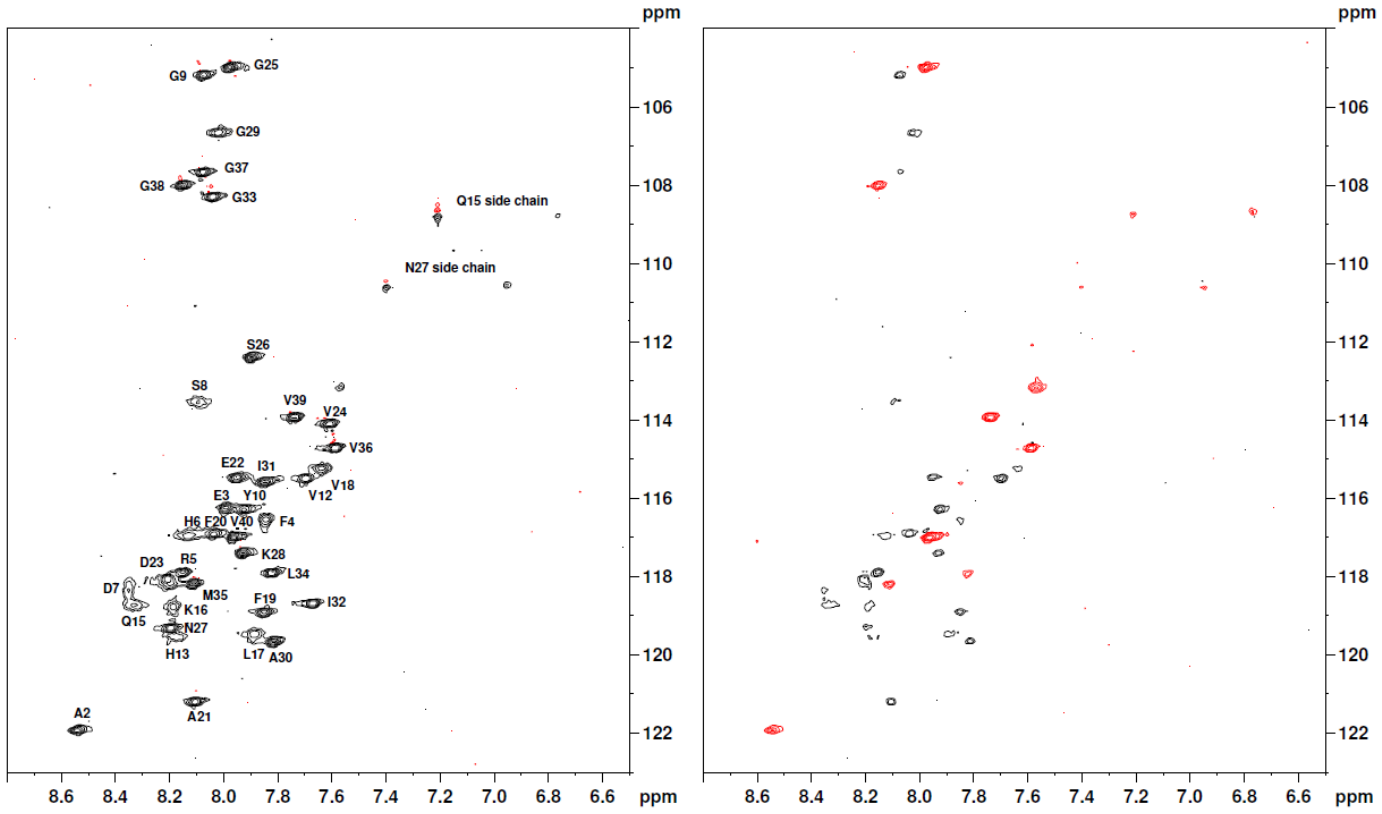

^{1}H-^{15}N HSQC Spectra of $A\beta_{1\text{-}40}$ in 100% $DMSO_{d6}$ without (left panel) and with (right panel) application of the heteronuclear NOE. In the right panel, positive peaks are plotted as black contours and negative peaks are plotted in red.

Sup. Fig. 7 Comparsion of ^{1}H-^{15}N NOE ratio of $A\beta_{1\text{-}40}$ in water and $DMSO_{d6}$.

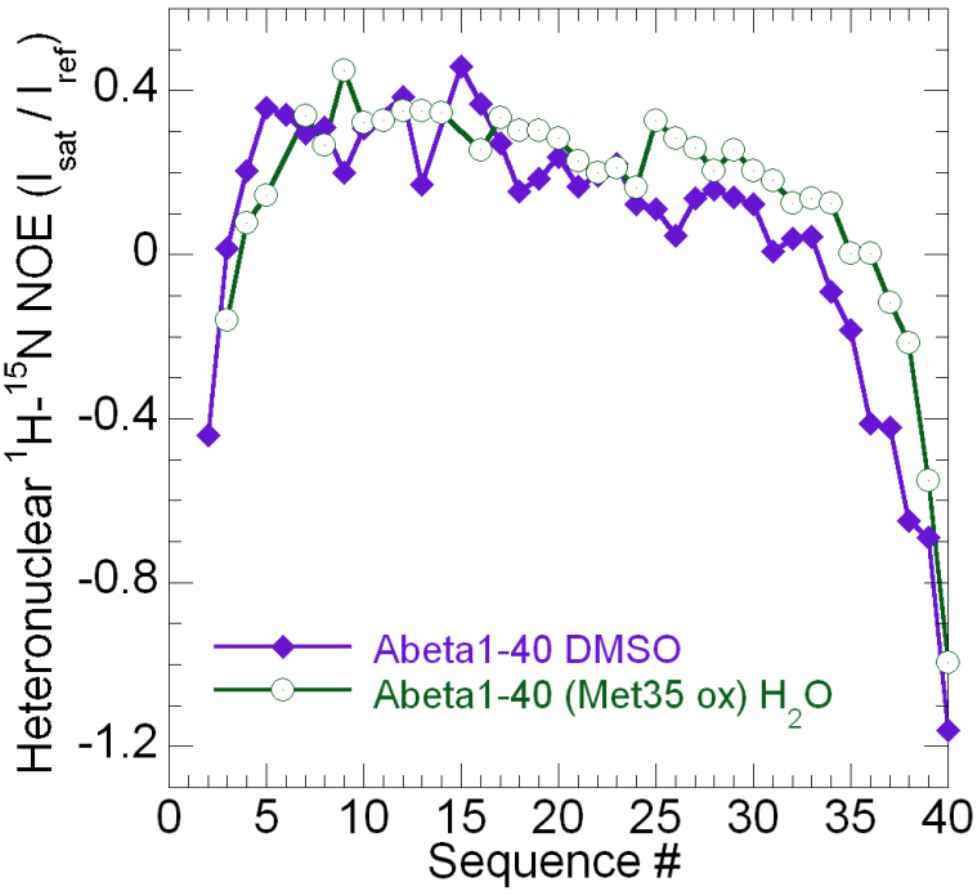

Comparison of the peak integrals with and without application of the ^{1}H-^{15}N heteronuclear NOE. **Purple** diamonds, this work in $DMSO_{d6}$; **Green** open circles, Riek *et al.* (2001) in aqueous solution.

Sup. Fig. 8

H/D exchange of Aβ preincubated in DMSO and diluted 20 fold into D_2O containing 5 mM Na/D Ac_{d3} buffer (pH* 4.52) at 5ºC. The table below shows the observed exchange rate obtained by fitting an exponential decay function to the data.

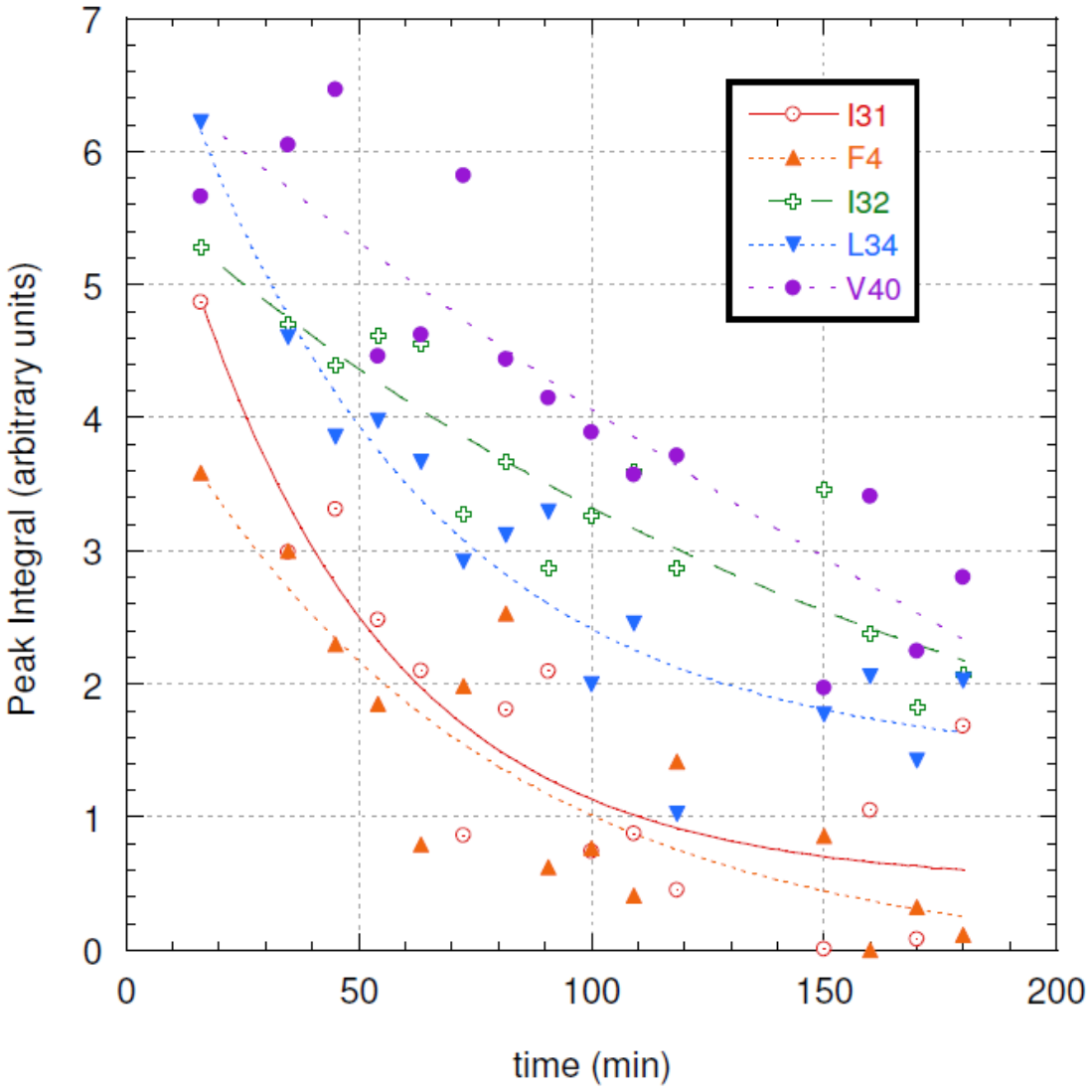

Residue	k_{obs} (min^{-1})	R
Ile 31	0.023 ± 0.007	0.91
Phe 4	0.014 ± 0.007	0.88
Ile 32	0.006 ± 0.005	0.92
Leu 34	0.018 ± 0.004	0.95
Val 40	0.0057 ± 0.0009	0.90

Sup. Fig. 9 Thioflavin T Assay for Amyloid-like Conformers.

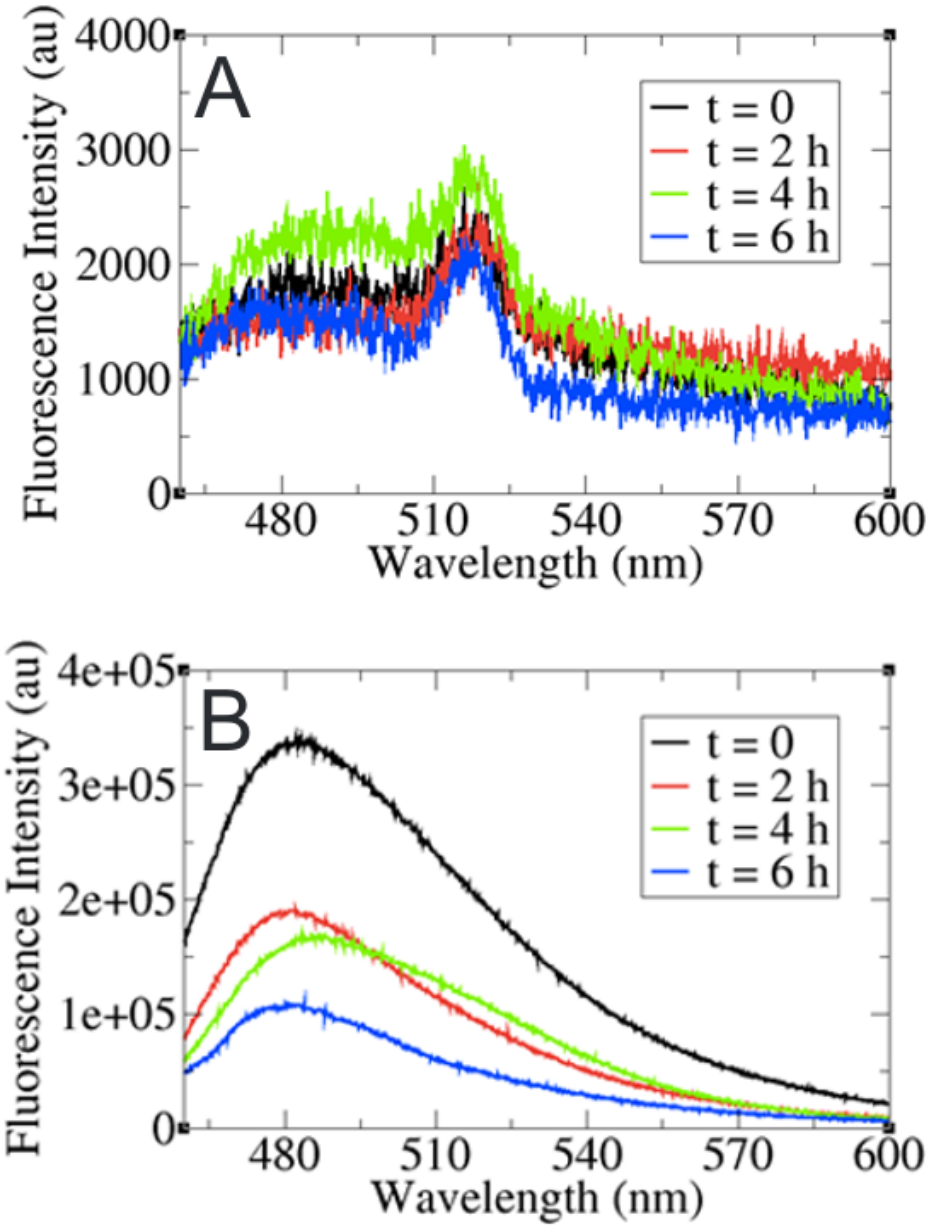

Thioflavin T fluorescence of 25 μM $A\beta_{1\text{-}40}$ in DMSO (*panel **A***) and H_2O (*panel **B***), at 30 ºC. In DMSO, the peptide is in its monomeric form as indicated by the absence of a strong fluorescence enhancement at 482 nm

upon dilution into ThT containing buffer. Evolution over time is consistent with the lack of amyloid-like conformers. In contrast, following incubation in aqueous solution (*panel B*) a strong increase in ThT fluorescence emission is observed, which is consistent with the presence of amyloid-like conformers. The decreasing intensity signal over time may arise from slow precipitation of $A\beta_{1\text{-}40}$ aggregates.

Sup. Fig. 10 1D ^{1}H NMR Spectra of Aβ and Inhibitor Compounds.

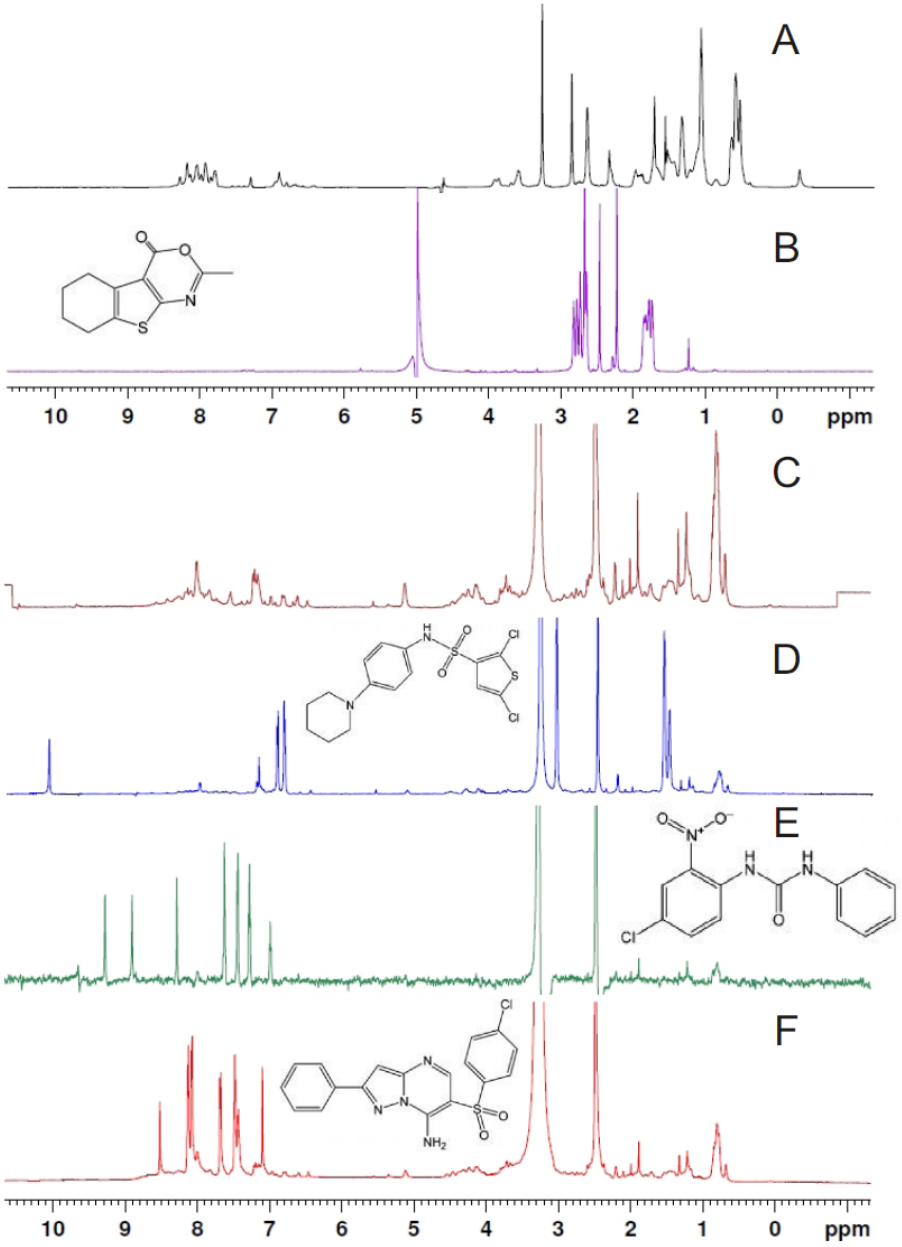

1D ^{1}H NMR spectra of $A\beta_{1\text{-}40}$ in **A**. 90%H_2O/10%D_2O pH 7, 5ºC either alone **A**. (**black** spectrum) or **B**. with a large excess of 2-methyl-5,6,7,8-tetrahydro-4H-[1]benzothieno[2,3-d][1,3]oxazin-4-one (compound 1, **purple** spectrum). The H_2O signal was suppressed using a Watergate module.

1D ^{1}H NMR spectra of $A\beta_{1\text{-}40}$ in 100% $DMSO_{d6}$ 30ºC alone **C**. (**brown** spectrum) or in the presence of a large excess of **D**. 2,5-dichloro-N-(4-peperidinophenyl)-3-thiophenesulfonamide (compound 2 **blue** spectrum); **E**. N-(4-chloro-2-nitrophenyl)-N'-phenylurea (compound 3, **green** spectrum) or **F**. 6-[(4-chlorophenyl)sulfonyl]-2-phenylpyrazolo[1,5-a]pyrimidin-7-amine (compound 4. **red** spectrum). The intense

peaks at 3.3 and 2.5 ppm in panels C, D, E and F arise from H_2O and penta-deuterated, mono-hydrogenated DMSO ($DMSO_{d5h1}$), respectively.

Sup. Fig. 11A

2D ^{1}H-^{15}N HSQC Spectra of Aβ alone or in the presence of C1 in **aqueous solution.**

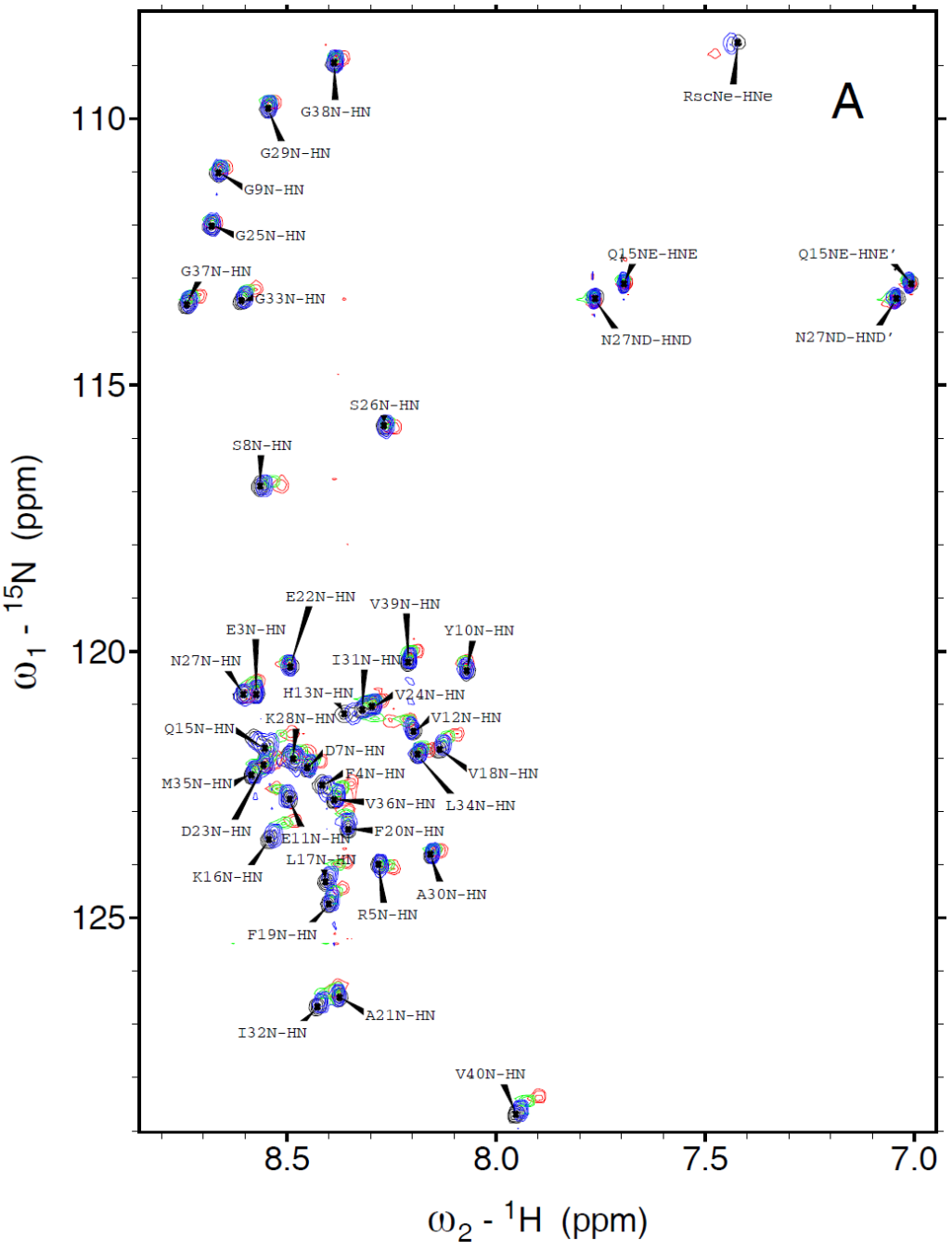

$A\beta_{1\text{-}40}$ peaks without (**black**) and with one (**blue**), three (**green**) and five (**red**) equivalents of C1. All peaks are plotted as contours separated by a multiplication factor of two.

Sup. Fig. 11B

2D ^{1}H-^{15}N HSQC Spectra of Aβ alone or in the presence of C1 in neat **$DMSO_{d6}$.**

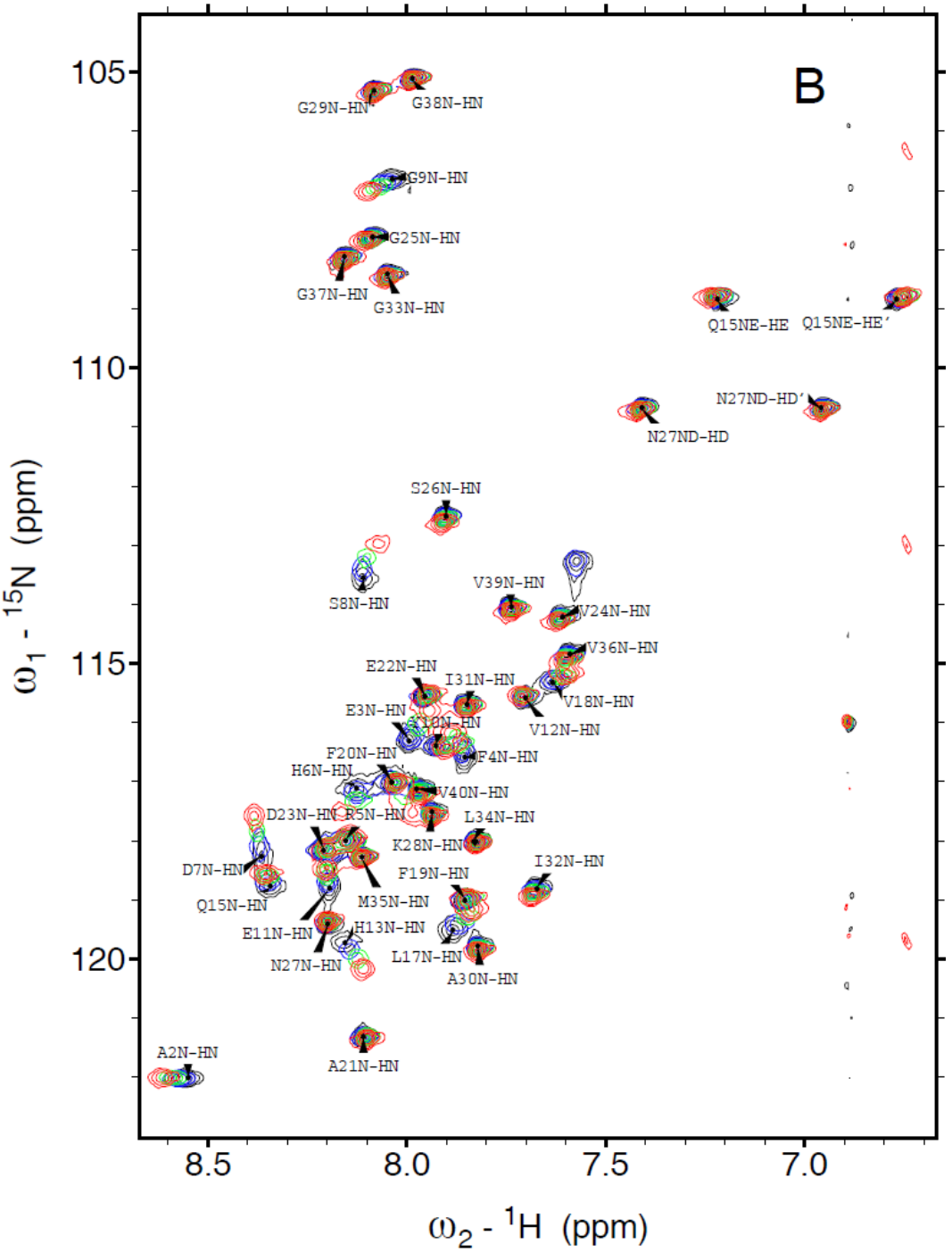

$A\beta_{1\text{-}40}$ peaks without (**black**) and with one (**blue**), three (**green**) and five (**red**) equivalents of C1. All peaks are plotted as contours separated by a multiplication factor of two.

Supporting Figure 12

^{1}H-^{15}N Aβ Chemical Shift Changes Induced by C2 (**A**), C3 (**B**) and C4 (**C**) in $DMSO_{d6}$

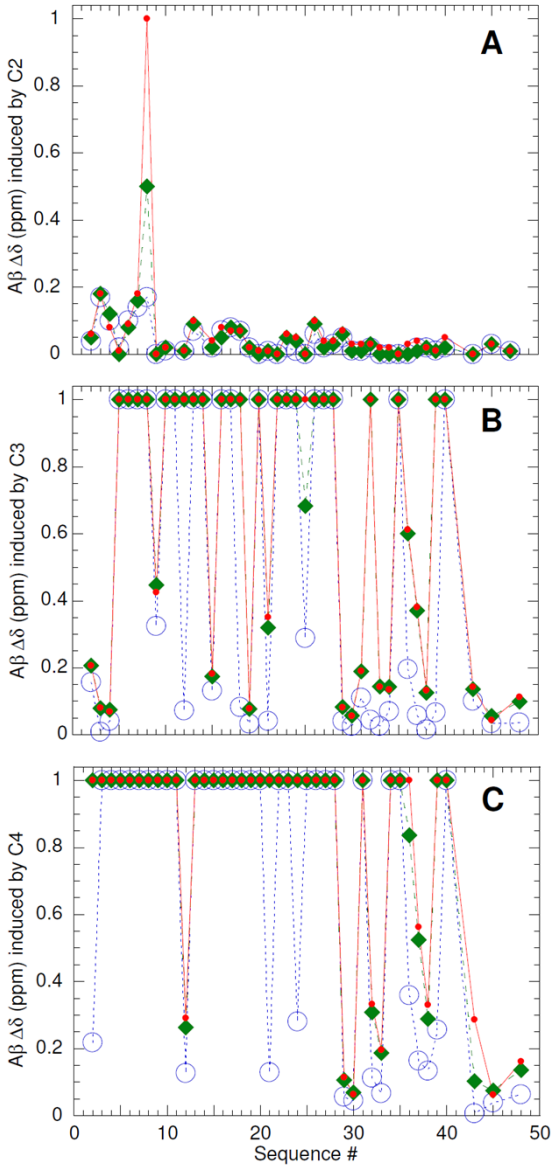

The weighted average shift changes for ^{1}H and ^{15}N nuclei in the presence of 1 eq of inhibitor (large open blue circles, dotted line), 3 eq inhibitor (green diamonds, dashed lines) and 5 inhibitor (small red circles) were calculated as reported in the **Methods** section. The data at sequence # 42, 45/46 and 48/49 correspond to the side chain groups of R5, Q15 and N27, respectively